Catalysis Today 164 (2011) 46–51

Contents lists available at ScienceDirect

Catalysis Today

journal homepage: www.elsevier.com/locate/cattod

Time-resolved in situ UV/vis spectroscopy for analyzing the dynamics of surface and bulk redox processes in materials used as oxygen storage capacitors

Evgenii V. Kondratenko[a,*], Yoshiyuki Sakamoto[b], Kohei Okumura[b], Hirofumi Shinjoh[b]

[a] Leibniz Institute for Catalysis at the University of Rostock, Albert-Einstein-Str. 29A, Rostock D-18059, Germany
[b] Toyota Central R&D Labs., Inc. 41-1, Aza Yokomichi, Oaza Nagakute, Nagakute-cho, Aichi-gun, Aichi-ken 480-1192, Japan

ARTICLE INFO

Article history:
Available online 10 November 2010

Key words:
Oxygen storage capacity
Dynamics
Redox
UV/vis analysis
Platinum
Ceria

ABSTRACT

Time-resolved UV/vis-DR (diffuse reflectance UV/vis) spectroscopy was used to in situ monitor the dynamics of reduction and reoxidation of Pt-free and Pt-containing CeO_2–ZrO_2 used as oxygen storage capacitors. This method can be also applied for measuring the speed of oxygen release. Combining the spectroscopic catalyst characterization with transient reaction analysis (alternating feeding of $CO(H_2)$ and O_2) enabled us to identify factors determining surface and bulk redox processes of ceria. The presence of Pt increased strongly the mobility and availability of lattice oxygen in CeO_2–ZrO_2 for oxygen release reactions, while the presence of strongly polymerized CeO_x species (non-homogeneous distribution of ZrO_2 in CeO_2) decreased the mobility of lattice oxygen. The results of the present in situ UV/vis-DR analysis support previous non-directly derived conclusions.

1. Introduction

Three-way catalysts show their highest performance for the removal of HC (hydrocarbons), CO, and NO_x from automotive exhaust gases at the air-to-fuel ratio close to 14.6 [1,2]. To keep this ratio over the catalyst surface, materials possessing high oxygen storage capacity (OSC) are required. Ceria–zirconia solid solutions are widely used as oxygen storage capacitors [3–13]. OSC is defined as the amount of oxygen stored by catalytic materials and provided for oxidation of HC and CO. There are three classical methods for determining OSC: (i) temperature-programmed reduction with CO or H_2, (ii) CO or H_2 pulse experiments with time resolution in seconds, and (iii) O_2 chemisorption at room temperature after catalyst reduction by H_2 at high temperatures. Sakamoto et al. [14] suggested a new method for determining OSC performance by measuring the amount of oxygen storage/release from planar catalysts on the millisecond scale using two CO pulses with millisecond pulse width. They concluded that the speed of oxygen release rather than the overall OSC values is an essential property of active OSC catalysts.

To the best of the author's knowledge, the dynamics of ceria reduction and oxidization was not in situ characterized during the OSC tests. This is a drawback for establishing the direct relationships between the OSC performance of solid materials and their physicochemical properties. In the present contribution, we demonstrate the potential of time-resolved diffuse reflectance UV/vis (UV/vis-DR) spectroscopy for in situ monitoring the reduction (with CO and H_2) and reoxidation (with O_2) of Pt-free and Pt-containing CeO_2–ZrO_2 with simultaneous determining their OSC performance. These materials differ in their OSC, as well as Pt and ZrO_2 distribution in CeO_2 [11,15]. In addition, we suggest that temporal changes in the Kubelka–Munk function in the range of absorption of reduced ceria (500–800 nm) can be used as a measure of the speed of oxygen release.

2. Experimental

2.1. Catalyst preparation and characterization

Three CeO_2–ZrO_2 (CZ-O, CZ-D, and CZ-R) supports with a molar ratio of Ce/Zr = 1 were prepared according to the procedure in Ref. [11]. Briefly, CZ-O was synthesized by precipitating a fine ceria powder (ANA KASEI Co. Ltd., 99.9% purity) using $Zr(OH)_4$ (Wako Pure Chemical Industries, Ltd.) by hydrolysis of $ZrO(NO_3)_2$ (Wako Pure Chemical Industries, Ltd.) with aqueous NH_3. Then, the solid was dried at 663 K and finally calcined at 773 K for 5 h in air. CZ-R was prepared by the same procedure as CZ-O, except that it was first reduced at 1473 K for 4 h by CO and then reoxidized at 773 K for 3 h in air. CZ-D was synthesized via a mechano-chemical reaction of CeO_2 and ZrO_2 powders in a high-energy ball mill. Pt/CZ-O, Pt/CZ-R, and Pt/CZ-D were prepared by conventional impregnation of the supporting materials with a $Pt(NH_3)_2(NO_2)_2$ (Tanaka Kikinzoku Kogyo K.K.) solution to give Pt content of 1.0 wt.%. Thereafter, the samples were calcined at 773 K for 3 h in air.

* Corresponding author. Tel.: +49 381 1281 290; fax: +49 381 1281 51290.
E-mail address: evgenii.kondratenko@catalysis.de (E.V. Kondratenko).

0920-5861/$ – see front matter © 2010 Elsevier B.V. All rights reserved.
doi:10.1016/j.cattod.2010.10.015

Nitrogen physisorption was employed to obtain specific surface areas in a single-point BET analyzer (Micro Sorb 4232 II, Micro Data Co., Ltd.). Pt dispersion was determined by CO chemisorption in a flow-type adsorption apparatus using CO pulses (OHKURA RIKE R6015-S). Pt particle sizes and the grain sizes of CeO_2–ZrO_2 were determined from X-ray diffraction analysis (RINT2200, Rigaku Co., Ltd., with Cu K radiation) using the Scherrer equation. More details on the catalyst characterization are provided in Refs. [11,15].

2.2. Oxygen storage capacity tests with in situ UV/vis-DR materials characterization

OSC performance of Pt-free and Pt-containing CeO_2-ZrO_2 materials was determined in a home-developed setup under isothermal conditions from transient ambient-pressure analysis of their reduction by CO (CO/Ar/Ne = 10/10/40) and H_2 (H_2/Ar/Ne = 10/10/40) followed by their reoxidation with O_2. Steady-state, time- (0.2 s time resolution) and spatial-resolved in situ UV/vis-DR catalyst characterization as well as catalytic tests in combination with isotopic traces can be run simultaneously from the same catalyst under identical reaction conditions [16]. A tubular fixed-bed quartz reactor (internal diameter 6 mm) was employed. The temperature within the catalyst bed was measured using an axially movable thermocouple located inside the quartz capillary. The catalyst quantity was fixed as approximately 200 mg. The catalyst sample (sieve fraction of 250–350 μm) was packed within the isothermal zone of the reactor between two layers of quartz particles of the same sieve fraction.

The OSC experiments were performed according to the following protocol. The catalyst was heated in an O_2 flow (O_2/Ne = 10/40, 50 $ml_{(STP)}$ min^{-1}) up to 623 K with a heating rate of 10 K min^{-1} at ambient pressure and tempered for 30 min. Thereafter, it was cooled down to 523 K in the same flow and flushed with Ne for 5 min to remove weakly adsorbed oxygen species. Then, a CO or H_2-containing mixture was fed to the catalyst for 20 min followed by Ne feeding for 5 min. Finally, the reduced catalyst was reoxidized in an O_2 feed (O_2/Ne = 10/40, 50 $ml_{(STP)}$ min^{-1}) for 20 min at the same temperature. Transient experiments at 573 and 623 K were carried out as described above.

The oxidation state of the catalysts was monitored by in situ UV/vis-DR spectroscopy using an AVASPEC fiber optical spectrometer (Avantes) equipped with a DH-2000 deuterium–halogen light source and a CCD array detector. $BaSO_4$ was used as a white reference material. UV/vis-DR spectra (from 200 to 800 nm) and the Kubelka–Munk function at 700 nm (transitions related to reduced CeO_x species) were recorded every 20, and 2 s, respectively. According to Ref. [17], we defined R_{rel} as the reflectance of reduced samples to that of the fully oxidized ones as given in Eq. (1). From this reflectance, we calculated the relative Kubelka–Munk function $F(R_{rel})$ according to Eq. (2). The Kubelka–Munk function of fully oxidized catalysts was calculated from the ratio of the reflectance of the oxidized sample to that of $BaSO_4$.

$$R_{rel} = \frac{R_{reduced\ sample}}{R_{oxidized\ sample}} \quad (1)$$

$$F(R_{rel}) = \frac{(1 - R_{rel})^2}{2 \times R_{rel}} \quad (2)$$

where $R_{reduced\ sample}$ and $R_{oxidized\ sample}$ are the reflectance of the reduced and oxidized catalysts relative to $BaSO_4$.

A quadrupole mass spectrometer (Baltzer Omni Star 200) was used for quantitative analysis of reactants and reaction products. Transient responses at the reactor outlet were monitored at the following atomic mass units (AMUs): 44 (CO_2), 40 (Ar), 32 (O_2), 28 (CO_2, CO), 18 (H_2O), 2 (H_2) and 20 (Ne). The concentration of feed components and reaction products was calculated from the respective AMUs using standard fragmentation patterns and sensitivity factors, which were determined separately in calibration experiments.

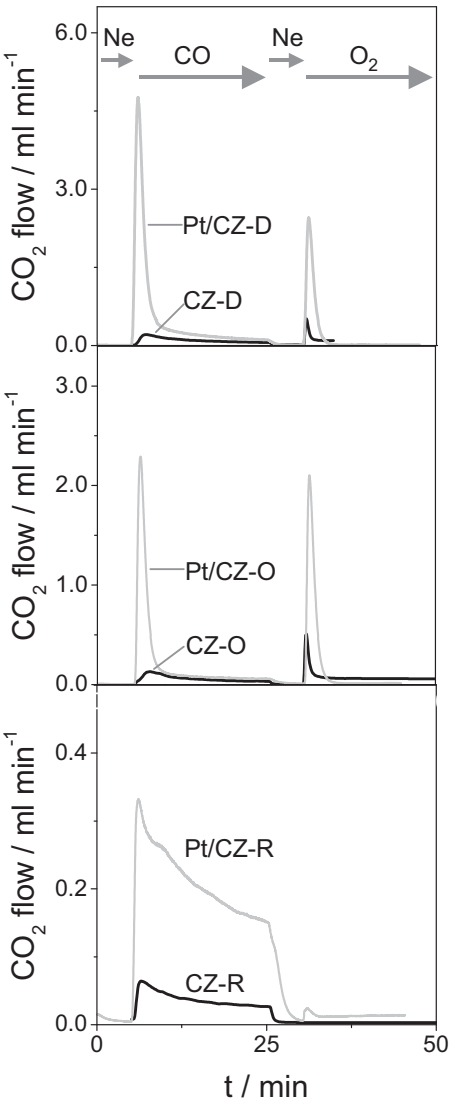

Fig. 1. Transient profiles of CO_2 formed during reduction and reoxidation of CZ-D, CZ-R, CZ-O, Pt/CZ-D, Pt/CZ-D, Pt/CZ-O, and Pt/CZ-R by CO (CO/Ar/Ne = 10/10/40) and O_2 (O_2/Ne = 20/80) at 523 K, respectively.

3. Results and discussion

3.1. Oxygen storage capacity from transient CO and H_2 experiments

Fig. 1 exemplifies transient CO_2 responses recorded during reduction of fully oxidized Pt-free and Pt-containing CeO_2–ZrO_2 by CO at 523 K and their subsequent reoxidation by O_2. In agreement with Refs. [18–21], the formation of CO_2 in the CO period proves that the oxidized catalysts provided their oxygen species for oxidizing CO to CO_2. The presence of CO_2 in the O_2 period can be explained by the fact that CO was stored on the catalyst surface as a carbonate intermediates as experimentally shown in Refs. [20–22] for $Ce_xZrO_{1-x}O_2$ ($0.15 \leq x \leq 1$). This intermediate was decomposed to gas-phase CO_2 in the O_2 period.

In order to calculate the OSC of the materials investigated, we integrated the CO_2 transients in the CO period. For compara-

Table 1
Amount of oxygen release calculated from H_2 consumed in the H_2 period and from CO_2 formed in the CO period over different materials at 523 and 623 K.

Materials	Oxygen release amount/mmol(O_2)/g(cat) calculated from H_2 consumption		Oxygen release amount/mmol(O_2)/g(cat) calculated from CO_2 formation	
	523 K	623 K	523 K	623 K
CZ-D		1.5	0.3	0.7
Pt/CZ-D	3.3	3.3	1.1	1.5
CZ-O		0.8	0.3	0.3
Pt/CZ-O	3.3	3.3	0.7	0.9
CZ-R		0.5	0.1	0.5
Pt/CZ-R	3.6	3.7	0.6	1.9

tive purposes, we computed the OSC values determined from the amount of H_2 consumed in the transient H_2 experiments performed according to the protocol described in Section 2.2. The results obtained are summarized in Table 1. The OSC values determined from CO oxidation are lower than those calculated from the H_2 consumption. This difference can be explained by the dissimilar acidic properties of CO_2 and H_2O formed from CO and H_2, respectively. Due to the lower acidity of H_2O, the removal of lattice oxygen from the catalysts via H_2O desorption should be easier than that via the CO_2 desorption. Another possible reason for the lower amount of oxygen release as CO_2 can be the fact that Pt is poisoned by CO and loses the catalytic activity [23]. Such a poisoning effect is not specific for H_2. Since higher temperatures favor CO desorption, the negative effect of CO decreases [24]. As a result, the difference between CO and H_2 for the oxygen removal from ceria diminishes, too (Table 1).

It is also important to mention that the OSC values of the Pt-free CeO_2–ZeO_2 are significantly lower than those of the Pt-containing ones. The improving effect of Pt agrees with the previous conclusions of Suda et al. [25]. The latter authors investigated the effect of Pt loading in ceria–zirconia solids on their OSC as determined from the catalyst reduction by H_2 using a thermo-gravimetric method. A possible mechanistic explanation of the accelerating effect of Pt is given in the following sections taking into account the results of in situ catalyst characterization by time-resolved UV/vis-DR.

3.2. *In situ UV/vis-DR analysis of redox behavior of ceria–zirconia*

The UV/vis-DR spectra of CZ-D, CZ-O, and CZ-R in an O_2 flow at 523 K are compared in Fig. 2(a). Despite the UV/vis-DR spectroscopy has limitations for interpreting large bandwidths, it has been often applied for investigating redox properties, surface coordination and polymerization degree of ceria-based materials [26–30] and other transitional metal oxides [17,31–36]. According to Ref. [26], the UV/vis-DR spectrum of pure CeO_2 is characterized by two broad absorption bands at 275 and 350 nm (charge transfer (CT) transitions from O^{2-} to Ce^{4+}). The oxidized CZ-O exhibits the CT bands at 272 and 347 nm indicating the presence of individual CeO_2 particles in this catalyst. It is also clearly seen from Fig. 2(a) that there is a slight shift in the absorption at 347 nm towards higher wavelength in the UV/vis-DR spectra of CZ-D, and CZ-R. A similar shifting was previously reported for CeO_2 promoted by SiO_2, ZrO_2, TiO_2, and HfO_2 [28–30]. This effect was explained by lowering symmetry in the CeO_2 lattice caused by substitution of cerium cations by other elements. In other words, this shifting can be considered as an indicator for the homogeneity of dissolving zirconia within ceria. For our samples, it can be concluded that CZ-O possesses big CeO_2 aggregates, while CZ-R and CZ-D are homogeneous solid solutions of CeO_2 and ZrO_2. This conclusion is in agreement with the results of previous thorough characterization of these catalysts [11,15]. The presence of Pt in CZ-D, CZ-O, and CZ-R does not influence the position of absorption bands below 400 nm. Some additional absorption bands appear in the range between 400–700 nm in the UV/vis-DR spectra of Pt/CZ-D and Pt/CZ-O. They might be related to 2–5 nm Pt particles, which dominate on the surface of these catalysts.

In order to derive fundamental insights into the dynamics of reduction and reoxidation of the Pt-free and Pt-loaded CeO_2–ZrO_2, we applied in situ UV/vis-DR spectroscopy for catalyst characterization during CO (H_2) and O_2 transient experiments, respectively. Fig. 2(b) exemplifies the UV/vis-DR spectra of CZ-D in an O_2 flow as well as after 5 and 10 min on stream in a CO feed at 523 K. The spectra were converted to the relative Kubelka–Munk (KM) function $F(R_{rel})$ according to Eqs. (1) and (2). No absorption bands are observed in the spectral range from 400 to 800 nm for the fully oxidized sample. When the sample was treated with CO, broad absorption band(s) appear between 500 and 800 nm and their intensity increases with the duration of the CO treatment. Very similar changes in the UV/vis-DR spectra were observed for all catalysts studied, when CO and H_2 were used as reducing agents. These changes are reversible after sample reoxidation by O_2 (O_2/Ne = 20/80). Therefore, they should be due to the redox behavior of ceria, since zirconia is not reduced at 523 and 623 K. The following discussion supports this conclusion.

Fig. 3 shows temporal changes in $F(R_{rel})$ at 700 nm and the CO_2 evolution during the reduction of CZ-D and CZ-R in CO followed by their subsequent reoxidation in O_2. It should be stressed that in these experiments we always started with the fully oxidized sam-

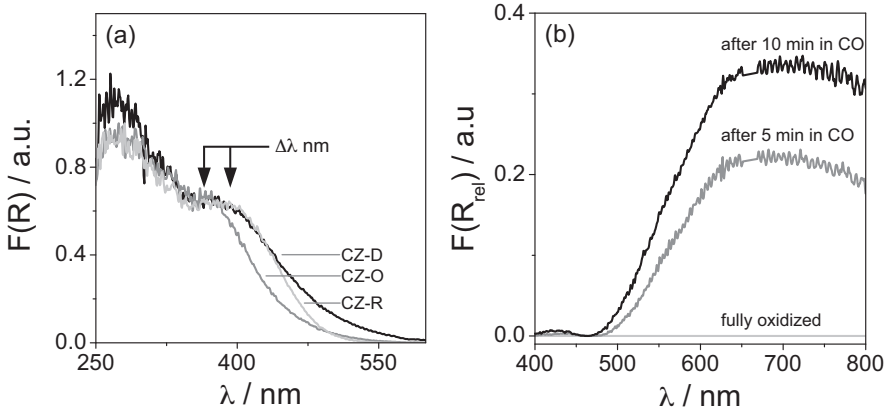

Fig. 2. UV/vis-DR spectra of (a) CZ-D, CZ-O, and CZ-R in an O_2 flow (O_2/Ne = 20/80) and (b) after 0, 5 and 10 min on stream in a CO feed at 523 K.

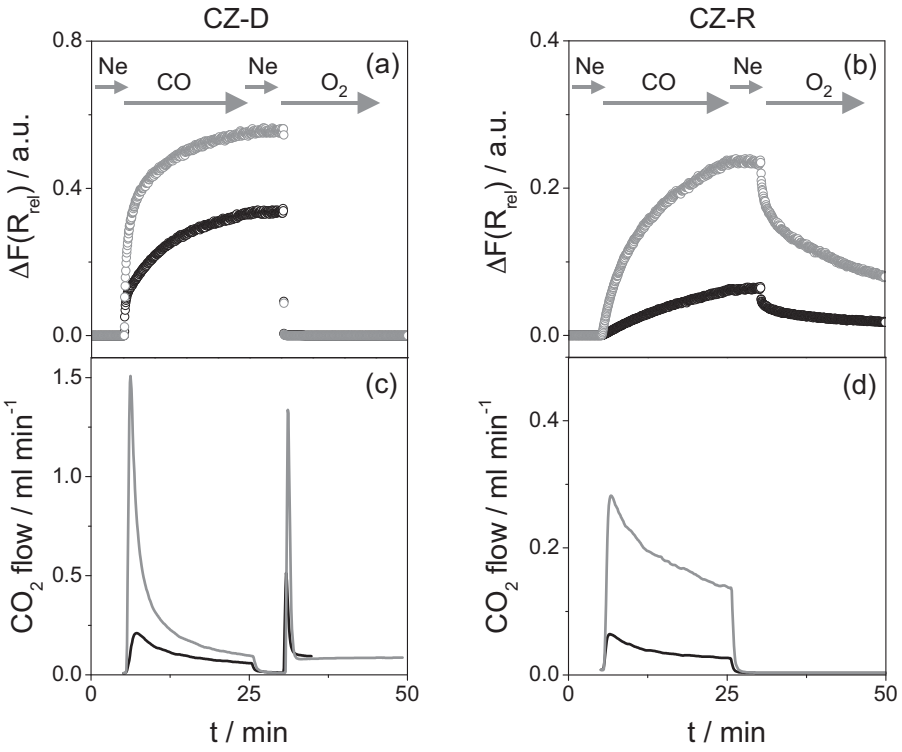

Fig. 3. Temporal changes in (a and b) the relative Kubelka–Munk function at 700 nm and in (c and d) the CO_2 formation during reduction and reoxidation of CZ-D and CZ-R by CO and O_2 at 523 (black symbols) and 623 K (grey symbols), respectively.

ples. In order to avoid CO oxidation in the presence of gas-phase O_2, the O_2-treated catalysts were flushed with pure Ne at the reaction temperature for 5 min before CO feeding. As proven by mass spectroscopic analysis, this was enough to remove completely gas-phase O_2 from the reactor with the catalyst. This means that the formation of CO_2 during the CO treatment was due to the reaction of gas-phase CO with oxygen species stored by the catalyst; i.e. in absence of gas-phase O_2. It is also important to stress that the amount of CO_2 formed in these experiments and the KM function at 700 nm increased with temperature. Therefore, the increase in the KM function in Fig. 3 upon switching from an O_2 flow to a CO flow can be ascribed to the reduction of Ce^{4+} to Ce^{3+} (ZrO_2 is not reduced at such low temperatures) due to the consumption of lattice oxygen for CO oxidation to CO_2. In order to prove whether the reduction/reoxidation of ceria is a reversible process, an O_2 flow (O_2/Ne = 20/80) was fed to the reduced sample (at ca. 30 min in Fig. 3) after its treatment in CO for 20 min. As shown in Fig. 3, the KM function at 700 nm falls to 0 after a few seconds in the O_2 flow. Since the temporal changes in this function are faster under oxidizing than under reducing conditions, it can be concluded that the catalyst reduction by CO is slower as its reoxidation by O_2. Similar conclusion is also valid when H_2 is used as a reducing agent.

As previously reported for pure CeO_2 [27], the intensity of bands related to the reduced ceria depends on the specific surface area; the higher the area, the high the intensity. Since our catalysts differ strongly in their surface areas, the magnitude of the changes in the KM function cannot be used for quantifying and comparing the degree of reduction between these different solids. However, these changes are useful for elucidating the effect of temperature and Pt-loading on the redox properties of individual CeO_2–ZrO_2.

3.3. Effect of Pt on oxygen storage capacity of CeO_2–ZrO_2

Fig. 4 shows that the KM function at 700 nm increased, when different Pt-containing CeO_2–ZrO_2 materials were reduced by CO and decreased upon the catalyst reoxidation by O_2. However, it is clearly seen that the values of the KM function were smaller than those observed in the Pt-free CeO_2–ZrO_2 (Fig. 3). This is surprising because the Pt-free CeO_2–ZrO_2 produced significantly less CO_2 (Table 1), i.e. a lower amount of lattice oxygen was removed and, therefore, a lower reduction degree of ceria should be achieved than in the Pt-containing ones. In addition, the KM changes in the Pt/CZ-O and Pt/CZ-D treated in CO at 523 and 623 K did not increase but decrease with rising temperature. Similar results were previously reported by Binet et al. [27] for reduction of pure CeO_2 by H_2 above 673 K. This was explained by reoxidation of the surface of CeO_2 via a migration of bulk oxygen species. When we reduced the Pt/CZ-R material possessing big Pt particles and the most homogeneous distribution of ZrO_2 in CeO_2, the KM function at 700 nm increased initially followed by a decrease when the catalyst was reduced in CO at 623 K (Fig. 4). This is also valid for the reduction of Pt/CZ-R in H_2 (the results are not shown for brevity).

The different redox behaviors of the Pt-containing CeO_2–ZrO_2 compared to the Pt-free CeO_2–ZrO_2 can be explained as following. The reduction of the latter materials primarily affects the near to surface ceria cations. In other words, these species are not in equilibrium to the bulk ones. The presence of Pt on the surface of ceria–zirconia solutions enables the migration of bulk oxygen species towards the surface. As a result, the surface is oxidized, while the bulk becomes reduced. This statement is supported by previous experimental data proving the participation of bulk oxygen in the Pt-containing materials in CO oxidation [11,37].

As suggested in Ref. [25], the enhancing effect of Pt loading on the OSC performance of ceria–zirconia solid solutions can be due to (i) oxidation of CO and H_2 over PtO_2 formed during oxidative sample treatment, and (ii) enhancing oxygen release from ceria–zirconia solid solutions. In order to estimate the relative contributions of the above two effects of Pt, we calculated the amount of oxygen in PtO_2 for each Pt containing catalysts. The surface area of Pt in each catalyst can be estimated from the Pt dispersion and the

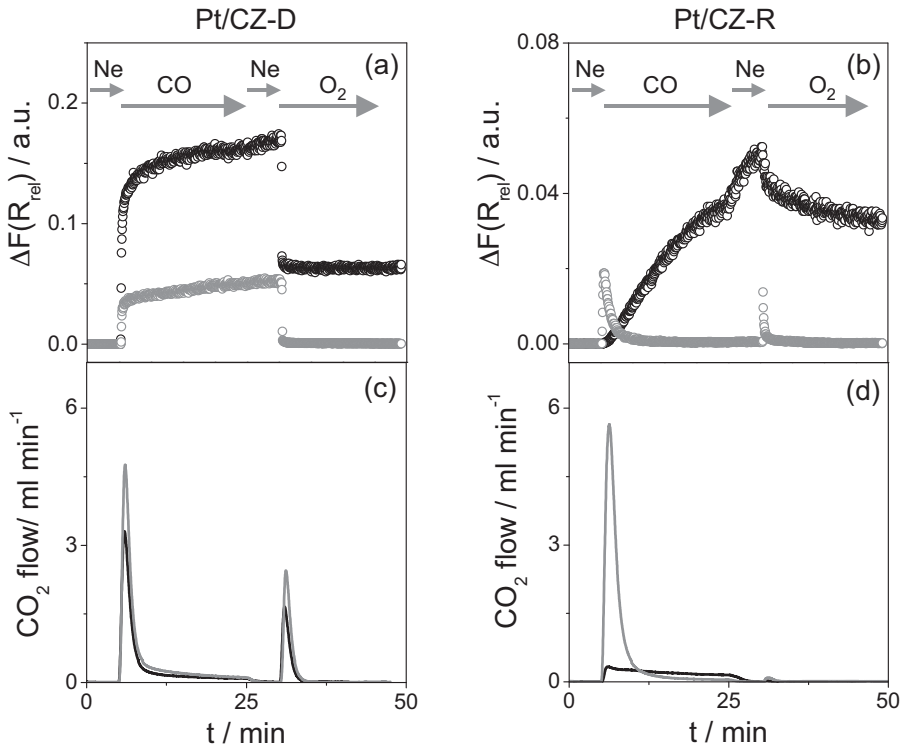

Fig. 4. Temporal changes in (a and b) the relative Kubelka–Munk function at 700 nm and in (c and d) the CO_2 formation during reduction and reoxidation of Pt/CZ-D and Pt/CZ-R by CO and O_2 at 523 (black symbols) and 623 K (grey symbols), respectively.

amount of Pt loading reported in previous papers [11,15]. The maximal possible amount of $CO_2(H_2O)$ formed via reduction of PtO_2 to Pt is equal to the number of surface Pt atoms multiplied by a factor of 2. The amount of oxygen in PtO_2 in Pt/CZ-D, Pt/CZ-O, and Pt/CZ-R was estimated to be 0.030, 0.012, and 0.001 mmol/g, respectively. Comparing these values with the overall amount of oxygen release calculated from H_2 consumption and CO_2 production in Table 1, we do not take into account the effect of oxidation of CO and H_2 over PtO_2 formed during oxidative sample treatment. Since the OSC values of Pt-containing catalysts are significantly higher than those of the Pt-free supports, it can be safely concluded that Pt increases the ability of ceria–zirconia for storage of oxygen species and, more important, for providing them for oxidation of reducing agents.

Finally, we discuss how to derive insights into the speed of oxygen release using the time-resolved in situ UV/vis-DR analysis. As demonstrated above, the magnitude of changes in the KM function in the range between 500 and 800 nm upon reduction and oxidation of ceria–zirconia oxygen capacitors depends on the specific surface area of the materials and is influenced by diffusion of oxygen from the bulk to the surface. Due to these facts, an absolute value of this function cannot be an indicator for quantifying the oxygen release speed. We suggest to use the time ($t_{1/2}$), which is required to achieve a half of the highest KM changes in the UV/vis-DR spectra of materials after switching from an oxidizing feed to a reducing one under isothermal conditions; the higher the $1/t_{1/2}$ value, the higher the speed of oxygen release. The corresponding values were calculated for all the materials studied and are plotted in Fig. 5. Irrespective of Pt loading, the $1/t_{1/2}$ increases with rising temperature proving that oxygen removal from ceria is an activated process. In agreement with the present and previous [25] results, our approach supports the higher activity of the Pt-containing materials compared to the Pt-free ones. With respect to the $1/t_{1/2}$ value, the latter materials can be ordered as follows: CZ-D > CZ-O > CZ-R. This order

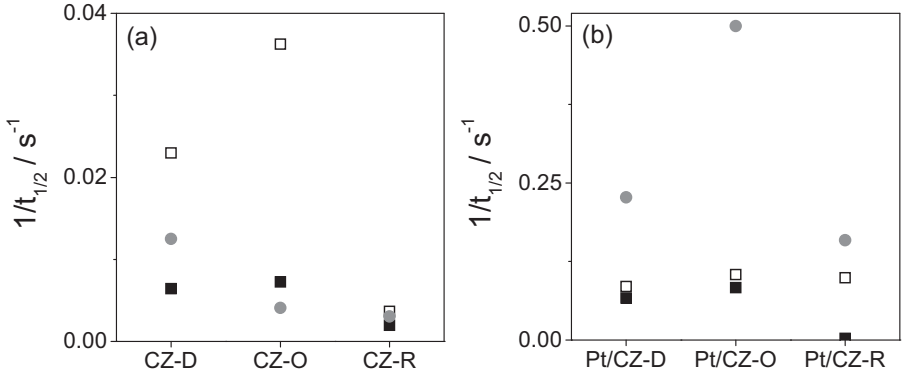

Fig. 5. Characteristic time ($1/t_{1/2}$) of the temporal changes in the Kubelka–Munk function at 700 nm after switching from O_2 flow to CO feed at 523 (■) and 623 K (□) or to an H_2 feed at 623 K (●) over (a) CZ-D, CZ-O, and CZ-R as well as (b) Pt/CZ-D, Pt/CZ-O, and Pt/CZ-R.

is also valid for the Pt-loaded ceria–zirconia at 523 K. However, $1/t_{1/2}$ increases more rapidly with temperature over the Pt/CZ-R material than over Pt/CZ-O and Pt/CZ-D. This agrees well with the temperature dependence of the initial rate for oxygen release as determined in Ref. [11].

4. Conclusions

In situ UV/vis-DR spectroscopy is suitable to follow the dynamics of reduction and oxidation of CeO_2–ZrO_2 used as oxygen storage capacitors. Moreover, this technique enables to discriminate between surface and bulk redox processes. The rate for ceria reduction by CO and H_2 was found to be slower than the rate of ceria reoxidation by O_2. The presence of Pt increases significantly the rate of the reduction and the amount of oxygen, which can react with reducing agents. The oxygen is supplied from the bulk of CeO_2–ZrO_2. Moreover, in contrast to classical OSC measurements, temporal analysis in the Kubelka–Munk function of reduced CeO_x species can provide a convenient indicator for the O_2 release speed without consideration of the readsorption of the product resulting on O_2 release process, like as CO_2 and H_2O, which hinder correct determining the O_2 release speed.

References

[1] S. Matsumoto, N. Miyoshi, T. Kanazawa, M. Kimura, M. Ozawa, in: S. Yoshida, T.N. Tabezawa, T. Ono (Eds.), Catalytic Science and Technology, vol. 1, Kodansha-VCH, Tokyo, 1991, p. 335.
[2] S. Matsumoto, H. Shinjoh, Adv. Chem. Eng. 33 (2008) 1.
[3] A. Trovarelli, F. Zamar, J. Llorca, C. de Leitenburg, G. Dolcetti, J.T. Kiss, J. Catal. 169 (1997) 490.
[4] A. Suda, T. Kandori, N. Terao, Y. Ukyo, H. Sobukawa, M. Sugiura, J. Mater. Sci. Lett. 7 (1998) 77.
[5] H. Vidal, S. Bernal, J. Kaspar, M. Pijolat, V. Perrichon, G. Blanco, J.M. Pintado, R.T. Baker, G. Colon, F. Fally, Catal. Today 54 (1999) 93.
[6] A. Holmgren, B. Andersson, D. Duprez, Appl. Catal. B 22 (1999) 215.
[7] C.E. Hori, A. Brenner, S.K.Y. Ng, K.M. Rahmoeller, D. Belton, Catal. Today 50 (1999) 299.
[8] M. Boaro, C. de Leitenburg, G. Dolcetti, A. Trovarelli, J. Catal. 193 (2000) 338.
[9] H. Vidal, J. Kaspar, M. Pijolat, G. Colon, S. Bernal, A. Cordón, V. Perrichon, F. Fally, Appl. Catal. B 27 (2000) 49.
[10] S. Bedrane, C. Descorme, D. Duprez, Stud. Surf. Sci. Catal. 138 (2001) 125.
[11] T. Tanabe, A. Suda, C. Descorme, D. Duprez, H. Shinjoh, M. Sugiura, Stud. Surf. Sci. Catal. 138 (2001) 135.
[12] H. Vidal, J. Kaspar, M. Pijolat, G. Colon, S. Bernal, A. Cordón, V. Perrichon, F. Fally, Appl. Catal. B 30 (2001) 75.
[13] J. Fan, X. Wu, X. Wu, Q. Liang, R. Ran, D. Weng, Appl. Catal. B 81 (2008) 38.
[14] Y. Sakamoto, K. Kizaki, T. Motohiro, Y. Yokota, H. Sobukawa, M. Uenishi, H. Tanaka, M. Sugiura, J. Catal. 211 (2002) 157.
[15] F. Dong, A. Suda, T. Tanabe, Y. Nagai, H. Sobukawa, H. Shinjoh, M. Sugiura, C. Descorme, D. Duprez, Catal. Today 93–95 (2004) 827.
[16] E.V. Kondratenko, Catal. Today 157 (2010) 16.
[17] M.D. Argyle, K. Chen, C. Resini, C. Krebs, A.T. Bell, E. Iglesia, J. Phys. Chem. B 108 (2004) 2345.
[18] N. Hickey, P. Fornasiero, J. Kaspar, J.M. Gatica, S. Bernal, J. Catal. 200 (2001) 181.
[19] S. Hilaire, X. Wang, T. Luo, R.J. Gorte, J. Wagner, Appl. Catal. A 215 (2001) 271.
[20] M. Boaro, F. Giordano, S. Recchia, V.D. Santo, M. Giona, A. Trovarelli, Appl. Catal. B 52 (2004) 225.
[21] C. Descorme, R. Taha, N. Mouaddib-Moral, D. Duprez, Appl. Catal. A 223 (2002) 287.
[22] M. Zhao, M. Shen, J. Wang, J. Catal. 248 (2007) 258.
[23] B. Atalik, D. Uner, J. Catal. 241 (2006) 268.
[24] O. Dulaurent, D. Bianchi, Appl. Catal. A 196 (2000) 271.
[25] A. Suda, K. Yamamura, H. Sobukawa, Y. Ukyo, T. Tanabe, J. Ceram. Soc. Jpn. 112 (2004) 623.
[26] A. Bensalem, J.C. Muller, F. Bozon-Verduraz, J. Chem. Soc. Faraday Trans. 88 (1992) 153.
[27] C. Binet, A. Badri, J.-C. Lavalley, J. Phys. Chem. 98 (1994) 6392.
[28] B.M. Reddy, A. Khan, Catal. Surv. Asia 9 (2005) 155.
[29] B.M. Reddy, P. Bharali, P. Saikia, S.-E. Park, M.W.E. van den Berg, M. Muhler, W. Grünert, J. Phys. Chem. C 112 (2008) 11729.
[30] B.M. Reddy, P. Bharali, P. Saikia, G. Thrimurthulu, Y. Yamada, T. Kobayashi, Ind. Eng. Chem. Res. 48 (2009) 453.
[31] A. Bensalem, B.M. Weckhuysen, R.A. Schoonheydt, J. Phys. Chem. B 101 (1997) 2824.
[32] B.M. Weckhuysen, R.A. Schoonheydt, Catal. Today 49 (1999) 441.
[33] X. Gao, S.R. Bare, J.L.G. Fierro, I.E. Wachs, J. Phys. Chem. B 103 (1999) 618.
[34] E. Berrier, O. Ovsitser, E.V. Kondratenko, M. Schwidder, W. Grünert, A. Brückner, J. Catal. 249 (2007) 67.
[35] E.L. Lee, I.E. Wachs, J. Phys. Chem. C 111 (2007) 14410.
[36] O. Ovsitser, M. Cherian, A. Brückner, E.V. Kondratenko, J. Catal. 265 (2009) 8.
[37] E.V. Kondratenko, Y. Sakamoto, K. Okumura, H. Shinjoh, Appl. Catal. B 89 (2009) 476.